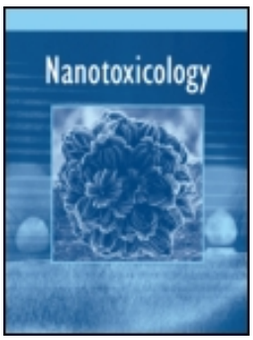

Nanotoxicology

ISSN: 1743-5390 (Print) 1743-5404 (Online) Journal homepage: https://www.tandfonline.com/loi/inan20

Transport of metal oxide nanoparticles and single-walled carbon nanotubes in human mucus

Ashish Jachak, Samuel K Lai, Kaoru Hida, Jung Soo Suk, Nina Markovic, Shyam Biswal, Patrick N. Breysse & Justin Hanes

To cite this article: Ashish Jachak, Samuel K Lai, Kaoru Hida, Jung Soo Suk, Nina Markovic, Shyam Biswal, Patrick N. Breysse & Justin Hanes (2012) Transport of metal oxide nanoparticles and single-walled carbon nanotubes in human mucus, Nanotoxicology, 6:6, 614-622, DOI: 10.3109/17435390.2011.598244

To link to this article: https://doi.org/10.3109/17435390.2011.598244

Published online: 29 Jul 2011.

Nanotoxicology, September 2012; 6(6):614–622

ISSN: 1743-5390 print / 1743-5404 online
DOI: 10.3109/17435390.2011.598244

informa
healthcare

ORIGINAL ARTICLE

Transport of metal oxide nanoparticles and single-walled carbon nanotubes in human mucus

Ashish Jachak[1], Samuel K Lai[2], Kaoru Hida[3], Jung Soo Suk[3], Nina Markovic[4], Shyam Biswal[1], Patrick N. Breysse[1] & Justin Hanes[5]

[1]Department of Environmental Health Sciences, The Johns Hopkins Bloomberg School of Public Health, Baltimore, Maryland, USA, [2]Department of Chemical and Biomolecular Engineering, The Johns Hopkins University, Baltimore, Maryland, USA, [3]Department of Biomedical Engineering, The Johns Hopkins University School of Medicine, Baltimore, Maryland, USA, [4]Department of Physics and Astronomy, The Johns Hopkins University, Baltimore, Maryland, USA and [5]The Center for Nanomedicine and the Wilmer Eye Institute, The Johns Hopkins University School of Medicine, Baltimore, Maryland, USA

Abstract

Whether mucus layers lining entrance points into the body, including the lung airways, provide protection against the penetration of engineered nanoparticles remains poorly understood. We measured the diffusion coefficients of hundreds of individual nanoparticles of three different metal oxides (nMeOs) and two types of single-walled carbon nanotubes (SWCNTs) in undiluted human mucus. We found that the vast majority of these nanoparticles are efficiently trapped in human mucus and, further, that the mechanism of trapping is adhesive interactions as opposed to steric obstruction. However, a small fraction of zinc oxide (ZnO) nanoparticles moved at rates fast enough to penetrate airway mucus layers. We conclude that human mucus layers probably provide considerable protection for mucosal tissues from the penetration of most nMeOs and SWCNTs, and suggest that further investigation of the potential health risks of exposure to ZnO nanoparticles is warranted.

Keywords: Nanotoxicology, lung, mucous membranes, reactive oxygen species

Introduction

Metal oxide nanoparticles (nMeOs), a class of engineered nanoparticles, offer unique metallic, semiconductor and insulator characteristics that have resulted in their wide adoption in chemical, electrical, optical and material science applications, including microelectronic circuits, sensors, fuel cells, anti-corrosive coatings and catalysts (Fernandez-Garcia et al. 2004). Three commercially manufactured and widely used nMeOs are oxides of cerium, zinc and zirconium. Cerium oxide (CeO_2) transmits visible light and absorbs ultraviolet (UV) light, and converts harmful gases to relatively non-harmful ones. Thus, CeO_2 is increasingly explored for uses in sunscreens and in catalytic converters (Deshpande et al. 2005). Zinc oxide (ZnO), an effective antibacterial agent, has been used in textiles (Li et al. 2007), food packaging, baby powders, shampoos, bandage tapes and antiseptic ointments (Padmavathy & Vijayaraghavan 2008). ZnO is also used in sunscreens (blocker for UV-A and UV-B radiation) (Markovic & Rerek 2002), solar cells and liquid crystal displays. Zirconium dioxide (ZrO_2) is used as a thermal barrier coating in jet and diesel engines, and in dental applications (Papaspyridakos & Lal 2008).

Carbon nanotubes (CNTs), due to their tensile strength, high conductivity, high surface area-to-volume ratio and unique electronic properties, are manufactured in substantial quantities for use in electronic devices and high-strength materials (Subramoney 1998; Sinnott & Andrews 2001). More recently, the applicability of single-walled carbon nanotubes (SWCNTs) has been explored as scaffolds in bone-tissue engineering, chromatographic purifications and antioxidant functionality (Niyogi et al. 2001; Shi et al. 2006, 2007; Sitharaman et al. 2007; Liu et al. 2009; Lucente-Schultz et al. 2009). However, concerns have been raised about toxicity related to CNT exposure in industrial settings. SWCNTs have been shown to enter cells (Bottini et al. 2006) and induce inflammation, reactive oxygen species (ROS), oxidative stress, DNA damage (Kisin et al. 2007; Pacurari et al. 2008) and cytotoxicity (Lam et al. 2004; Warheit et al. 2004; Risom et al. 2005; Shvedova et al. 2005, 2008b). Animal studies have also shown that SWCNTs cause transient inflammation, granulomas, lung lesions, alveolar wall thickening, interstitial fibrosis and reduced bacterial clearance (Lam et al. 2004; Warheit et al. 2004; Shvedova et al. 2008a, b).

As the production of engineered nanoparticles are scaled to meet their increasing demand, the potential for

Correspondence: Justin Hanes, The Center for Nanomedicine and the Wilmer Eye Institute, The Johns Hopkins University School of Medicine, 400 N. Broadway Street, Baltimore, MD 21231, USA. Tel: +410-614-6513. Fax: +410-614-6509. E-mail: hanes@jhu.edu

(Received 29 November 2010; accepted 15 June 2011)

occupational exposure to ambient nanoparticles increases. There has been substantial interest in nanomaterials-induced toxicity over the past decade, especially that caused by non-biodegradable materials, as summarized in several recent reviews (Hoet et al. 2004; Nel et al. 2006; Hirano 2009). Nevertheless, much remains to be understood about the health risks posed by non-biodegradable nanoparticles to the lung. While inhaled nanoparticles are capable of deposition throughout the human respiratory tract, nearly a third can deposit in the tracheobronchial region (generations G0–G16) (Kleinstreuer & Zhang 2010). The tracheobronchial airways are coated with a layer of viscoelastic mucus gel that is ~7–55 μm thick (Verkman et al. 2003). The mucus secretions, composed of entangled and crosslinked mucin fibres, offer a dense mesh network that can trap foreign particles by steric and/or adhesive interactions (Lai et al. 2007). Particles that are trapped in mucus are typically rapidly removed by mucus clearance mechanisms, thereby protecting the body against injury or infection by foreign particles. While mucus is generally considered an effective diffusional barrier against foreign particles, we recently discovered that some engineered nanoparticles, with surfaces mimicking those of viruses that infect mucosal tissues, can readily penetrate human mucus (Cone 2009). Thus, we sought to investigate whether CeO_2, ZrO_2, ZnO and SWCNT nanoparticles are capable of penetrating human mucus. We also measured nanoparticle-mediated toxicity to human bronchial epithelial cells in culture.

Methods

Preparation of fluorescent nMeOs and SWCNTs

In order to visualize the transport of nMeOs in mucus, the nanoparticles were functionalized to make them fluorescent. Fluorescent nMeOs were synthesized by the addition of primary amines, using aminopropyltriethoxysilane (APTES) to attach alkoxy silane groups to the surface hydroxyl groups (Xia et al. 2008). Once bound to the nanoparticles, the amines are available for the attachment of fluorescein isothiocyanate (FITC) molecules. Approximately 4 mg of the nMeOs were dispersed in 3 ml of anhydrous dimethylformamide (DMF). A solution of 0.5 μl APTES diluted in 25 μl DMF was added to the particle suspensions, sonicated and stirred under nitrogen at room temperature for 24 h. The modified nanoparticles were collected by centrifugation after removing the supernatant. After washing, the modified particles were resuspended in 0.5 ml DMF and mixed with a solution of 1 mg FITC in 0.5 ml DMF. The suspension was stirred for 4 h, and the FITC-labelled particles were collected by centrifugation. After thoroughly washing the labelled materials with DMF, the particles were dried under vacuum to remove the organic solvent. Fluorescently labelled particles were suspended in phosphate-buffered saline (PBS) for particle characterization and mucus experiments.

Due to strong inter-tube non-covalent interactions, SWCNTs are insoluble in organic, acidic or aqueous solvents (Chen et al. 2001); wrapping SWCNTs with anionic DNA improves their solubility (Zheng et al. 2003b; Becker et al. 2007) in aqueous media. Single-stranded DNA (ssDNA) may form π-stacking interactions with the side wall of CNTs (Zheng et al. 2003a). A suspension of well-dispersed SWCNTs was generated by wrapping SWCNTs with ssDNA (Becker et al. 2007). In order to visualize SWCNTs in mucus, we labelled the well-dispersed SWCNTs with fluorescent ssDNA (Alexa Fluor 488, AF488). Fluorescent ssDNA (Invitrogen, Inc., Carlsbad, CA, USA), was dissolved in ultrapure water to a final concentration of 1 mg/ml DNA. About 10 μl of each SWCNT (210 and 76 nm) solution was mixed with 90 μl of the AF488-labelled DNA solutions respectively. The mixed solutions were incubated at room temperature, in the dark, for 240 h. The solutions were concentrated using a forced air dialysis cell (Amicon, Millipore, Billerica, MA, USA) with a membrane molecular weight cut-off of 30 kDa to yield a higher concentration. The unattached DNA remaining in the solution was removed during the forced dialysis process (Becker et al. 2007). Synthetic, non-mucoadhesive particles that are densely conjugated with AF488 on the surface exhibited similar diffusion kinetics in mucus when compared with unmodified particles (data not shown), suggesting that AF488 labelling is unlikely to influence the mobility of labelled SWCNTs. The transport of fluorescent nMeOs and SWCNTs in mucus was compared with a positive control, a 500-nm fluorescent polystyrene particle with polyethylene glycol (molecular mass ≈ 2 kDa; Nektar Therapeutics, San Carlos, CA, USA) covalently attached to the surface (PS-PEG) (Lai et al. 2007).

Physicochemical characterization of nMeOs and SWCNTs

Cerium (IV) oxide (CeO_2, vendor-listed diameter <25 nm), ZnO (vendor-listed diameter <50 nm) and Zirconium (IV) dioxide (ZrO_2, vendor-listed diameter <100 nm) were purchased from Sigma Aldrich (St Louis, MO, USA). Sizes and ζ-potentials (surface charge) of fluorescent nMeOs, suspended in PBS, were determined using a Zetasizer Nano (Malvern Instruments, Southborough, MA, USA). Sizes and ζ-potentials of unlabeled, native nMeOs were also determined in DMEM/F12 (GIBCO BRL Life Technologies, Rockville, MD, USA), supplemented with 10% (v/v) foetal bovine serum and 1% antibiotics (penicillin-streptomycin), the same medium as the *in vitro* toxicity studies. The lengths of SWCNTs were characterized prior to use by atomic force microscopy (AFM) (Becker et al. 2007). The Zetasizer Nano was used to measure the ζ-potential of fluorescent SWCNTs suspended in PBS.

Collection of human cervicovaginal mucus

Human cervicovaginal mucus (CVM) was used as a surrogate for respiratory tract mucus. The biochemistry and rheological properties of human CVM are comparable to other mucus secretions, including the human respiratory tract (Lai et al. 2007). Human CVM is a readily available source of fresh undiluted human mucus. All experiments were performed in fresh, undiluted human CVM obtained from healthy volunteers with a self-sampling method approved by the Institutional Review Board at the Johns Hopkins University (Boskey et al. 2003). A mucus adsorbent was inserted into the vagina for 30 s, removed and placed into a 50 mL centrifuge tube that was centrifuged at 200× *g*

for 2 min to collect the secretions. Samples were collected from donors aged 19–26 years. Only non-ovulatory mucus was used in this study; ovulation can be visually determined by examining the spinnbarkeit of the mucus sample, which is increased significantly during ovulation. All mucus samples were used within a few hours and were kept at 4°C until used. The pH of human tracheobronchial mucus varies from 6.9 to 9.0, whereas the pH range of CV mucus from women with healthy vaginal microflora is around 4 (Boskey et al. 2003). In order to mimic tracheobronchial mucus, human CVM was neutralized to ~pH 7 by the addition of sodium hydroxide (5 M NaOH). Less than 3% v/v of NaOH was added to human CVM to minimize any dilution effects. Mucus samples were gently mixed to minimize any perturbations to the mucus structure. The initial and final pHs of all samples were confirmed by blotting onto pH paper.

Concentration of nMeOs and SWCNTs

Since concentration data from workplace monitoring for nMeOs was not readily available, a dose benchmark for mucus transport studies was based on the US Occupational Safety and Health Administration (OSHA) permissible exposure limits for CeO_2, ZnO and ZrO_2. The 8 h time-weighted average airborne concentration values were 15, 5 and 10 mg/m^3 respectively for CeO_2, ZnO and ZrO_2. We estimated the inhaled dose assuming an 8 h workday and the breathing rates (4.8 m^3/h) for healthy working adults (men) (EPA 1985). An expected approximation for deposited dose to the tracheobronchial region was then estimated using a 10% deposition fraction of the total inhalation dose, an estimate obtained for particles ≤100 nm from deposition models generated by the International Commission on Radiological Protection. The mass of nMeOs deposited on a daily basis in the tracheobronchial airways was calculated to be 58, 19 and 38 mg for CeO_2, ZnO and ZrO_2 respectively. Using the surface area of the tracheobronchial region (2471 cm^2) (Mercer et al. 1994), the dose per area was calculated. Based on these parameters, we estimated that human lung airways may be exposed to ~23, 8 and 16 μg/cm^2 of CeO_2, ZnO and ZrO_2 respectively on a daily basis. We used the peak mass concentration (53 μg/cm^3) (Maynard et al. 2004) of SWCNTs generated during the manufacturing process to determine the mass dose of SWCNTs. The mass dose of SWCNTs deposited in the tracheobronchial airways daily was calculated to be ~204 μg (mass per area dose of ~0.1 μg/cm^2).

Transport of nMeOs and SWCNTs in human CVM

In separate experiments, 3 μg of fluorescent nMeOs or SWCNTs suspended in PBS were added to ~30 μl of human CVM in a custom-made glass chamber (surface area of mucus chamber ≈ 0.3 cm^2) and incubated for 2 h prior to microscopy. This mass per unit area dose (3 μg ÷ 0.3 cm^2 ≈ 10 μg/cm^2) is representative of the mass dose of nMeOs that may deposit in the tracheobronchial airways of workers that inhale these particles. Particle suspensions were sonicated for 1 min prior to adding to mucus. Translational motions of fluorescent nMeOs and SWCNTs were recorded using an Electron Multiplying Charge Coupled Device (EMCCD) camera (Cascade II: 512; Photometrics, Tucson, AZ, USA) mounted on an inverted epifluorescence microscope (3-I Marianas; Zeiss, Thornwood, NY, USA) equipped with a 100× oil-immersion objective (numerical aperture 1.3). Movies were captured with Slidebook 4.2 Advanced Imaging Software (Olympus Soft Imaging Corp., Lakewood, CO, USA) at a temporal resolution of 66.7 ms for 20 s. The translational motions were analysed using Metamorph Software (Universal Imaging Corp., Downingtown, PA, USA) (Suh et al. 2003, 2005). Mean-squared displacements (MSD) and effective diffusivities (D_{eff}) were determined as previously described (Suh et al. 2003, 2005; Dawson et al. 2004). Three independent experiments in CVM from different donors, with $n \sim 100$ nanoparticles per experiment, were performed for each condition.

Penetration of nMeOs and SWCNTs in human CVM

To estimate the fraction of nMeOs or SWCNTs expected to penetrate human mucus layers of a given thickness, we used a numerical integration of Fick's second law. The model uses the effective diffusivity (D_{eff}) obtained from experimental data for each particle (Tang et al. 2009). We assumed a constant concentration of particles at the luminal mucus surface ($C_{x=0,t}=1$) and no particles within the mucus slab initially ($C_{x=0,t=0}=1$, $C_{0<x<\Delta L,t=0}=0$):

$$\frac{dC}{dt} = D_{eff}\frac{d^2C}{dx^2} \qquad (1)$$

where C is the concentration of particles, t is the time and x is the position. Briefly, the time-scale independent parameters for each individual particle (α and D_0) were obtained by fitting MSD to Equation (2).

$$MSD = 4D_0\tau^{\alpha} \qquad (2)$$

Using α and D_0, the time required for a particle to penetrate a given mucus thickness was calculated. The effective diffusivity for each particle was then calculated from Equation (3):

$$MSD = 4D_{eff}\tau \qquad (3)$$

The concentration profiles represent an arithmetic mean of the individual profiles for each particle type.

Cellular uptake of fluorescent nMeOs and SWCNTs

The human bronchial epithelial cell line, BEAS-2B, was maintained in DMEM/F12 (GIBCO BRL Life Technologies), supplemented with 10% (v/v) foetal bovine serum and 1% antibiotics (penicillin-streptomycin), at 37°C in a humidified atmosphere of air and 5% CO_2. About 1×10^5 BEAS-2B cells were plated in six-well plates and allowed to adhere overnight. Subsequently, the cells were incubated with 1 μg (surface area of each well is 9.6 cm^2; mass per area dose: 1 μg ÷ 9.6 cm^2 ≈ 0.1 μg/cm^2) of fluorescent nMeOs or SWCNTs for 4 h. Particle suspensions were sonicated for

1 min prior to particle addition. The supernatant was removed after 4 h, and cells were washed twice with PBS. Cells were collected for analysis using flow cytometry (FCM; BD Science, San Jose, CA, USA). Three independent experiments were performed.

Cellular toxicity of nMeOs and SWCNTs

BEAS-2B cell viability was measured by the MTT (3-(4-5-dimethylthiazol-2-yl)-2,5-diphenyltetrazolium bromide; Sigma Aldrich) assay. In this assay, the water-soluble yellow dye is readily internalized by viable cells and reduced by the action of mitochondrial dehydrogenases to an insoluble blue formazan product. BEAS-2B cells were seeded on 96-well tissue culture plates with 2×10^4 cells in 200 μl of media per well. After a 24-h adherence to the well surface and stabilization of the cells, they were treated with 10, 20, 30, 40 and 50 μg/ml (6.25–31.3 μg/cm^2) of nMeOs, suspended in cell culture medium, for 24 h. Particle suspensions were sonicated for 1 min prior to particle addition. At the end of exposure, 40 μl of MTT solution (2 mg/ml) was added and the cells were incubated for 4 h at 37°C. To dissolve the water-insoluble blue formazan product for colorimetric measurement, 200 μl of DMSO was used. The absorbance was quantified at 540 nm using a microplate spectrophotometer system (VersaMax; Molecular Devices, Sunnyvale, CA, USA). In a similar but separate experiment, the effects of SWCNTs on BEAS-2B cells were investigated at concentrations of 100, 200 and 400 μg/ml (25, 50 and 100 μg/cm^2). The viability of the treated group was expressed as the percentage of control group that was assumed to be 100%. Experiments were conducted in triplicate and each experiment was repeated three times.

Results

Physicochemical characterization of nMeOs and SWCNTs

Hydrodynamic diameters of fluorescent nMeOs, lengths of fluorescent SWCNTs and ζ-potentials for all fluorescent nanoparticles are presented in Table I. The sizes of fluorescent nMeOs in PBS were 495 ± 114, 114 ± 21 and 505 ± 29 nm for CeO_2, ZnO and ZrO_2 respectively. The primary particle diameters provided by the vendor were <25, <50 and <100 nm for CeO_2, ZnO and ZrO_2 respectively, suggesting that all three nMeOs experienced substantial agglomeration in solution, but less so for ZnO particles than CeO_2 and ZrO_2 particles. The surface charge (ζ-potentials) for fluorescent CeO_2, ZnO, ZrO_2, 76 nm SWCNTs and 210 nm SWCNTs were −16 ± 1, −9 ± 1, −23 ± 1, −9 ± 1 and −10 ± 1 mV respectively.

Transport of nMeOs and SWCNTs in human CVM

Time-lapse particle traces indicate that the motion of nMeOs and SWCNTs are greatly hindered by the mucus gel (Figure 1). Indeed, their traces are comparable to that of 500 nm uncoated, carboxylated polystyrene (PS-COOH) particles that are known to be adhesively trapped in human CVM (Lai et al. 2007). In contrast, 500 nm polystyrene (PS-PEG) particles coated with an extremely dense layer of low MW PEG exhibited freely diffusive traces that spanned microns in length (Lai et al. 2010). To quantify the motion of nMeOs and SWCNTs, we used multiple particle tracking, which allows us to quantify the motion of hundreds of individual nanoparticles, in the form of effective diffusivity (D_{eff}), with high spatial and temporal resolution (Suh et al. 2003, 2005; Dawson et al. 2004). Virtually, all nMeOs and SWCNTs were slowed compared with 500 nm PS-PEG nanoparticles, as evident by the distributions of D_{eff} for nMeOs and SWCNTs (Figure 2B–F) compared with D_{eff} for 500 nm PS-PEG particles (Figure 2A). Only ZnO particles had a small fraction of fast-moving particles that were capable of penetrating mucus at rates comparable to the majority of PS-PEG particles.

By fitting a mathematical model based on Fick's second law to the measured diffusion coefficients for hundreds of nanoparticles, we were able to estimate the fraction of nMeOs or SWCNTs that may penetrate a mucus gel layer. In the lung, estimates for the thickness of the luminal mucus gel range from 7 μm in the deep airways to 55 μm in the bronchi (Verkman et al. 2003). Assuming a thickness of 10 and 30 μm, we expect ~3% and 2% of the ZnO nanoparticles may penetrate the mucus layer within 1 h respectively (Figure 3A–B). Negligible fractions of CeO_2 and ZrO_2 (~0.3% and 0.0% respectively) particles are expected to penetrate a 10 μm thick mucus layer. We also found that virtually no SWCNTs (~0.0%) would penetrate a 10 μm thick mucus layer after 1 h (Figure 3A).

Based on the measured particle mobility, as well as assuming mucus to be 30 μm thick on average and a uniform particle deposition along the tracheobronchial airways, we estimated that ~380 μg of ZnO particles (2% of 19 mg deposited fraction) may reach the tracheobronchial epithelium in individuals exposed to ZnO at the OSHA exposure

Table I. Physicochemical properties of fluorescent metal oxide nanoparticles and single-walled carbon nanotubes.

Particle	Dimension measured	Dimensions of fluorescent nanoparticles (nm)	ζ-Potential of fluorescent nanoparticles (mV)
500 nm PS-PEG*	Diameter	529 ± 8	−5.6 ± 0.4
CeO_2†	Diameter	495 ± 66	−16 ± 1
ZnO†	Diameter	116 ± 10	−9 ± 1
ZrO_2†	Diameter	505 ± 17	−23 ± 1
210 nm SWCNT†§	Length	210 ± 48	−10 ± 1
76 nm SWCNT†§	Length	76 ± 27	−9 ± 1

*Data obtained from reference (Lai et al. 2007).
†Size and surface charge of fluorescent nanoparticles measured in phosphate-buffered saline.
§Length of SWCNTs measured by atomic force microscopy (Becker et al. 2007).
SWCNT, single-walled carbon nanotubes.

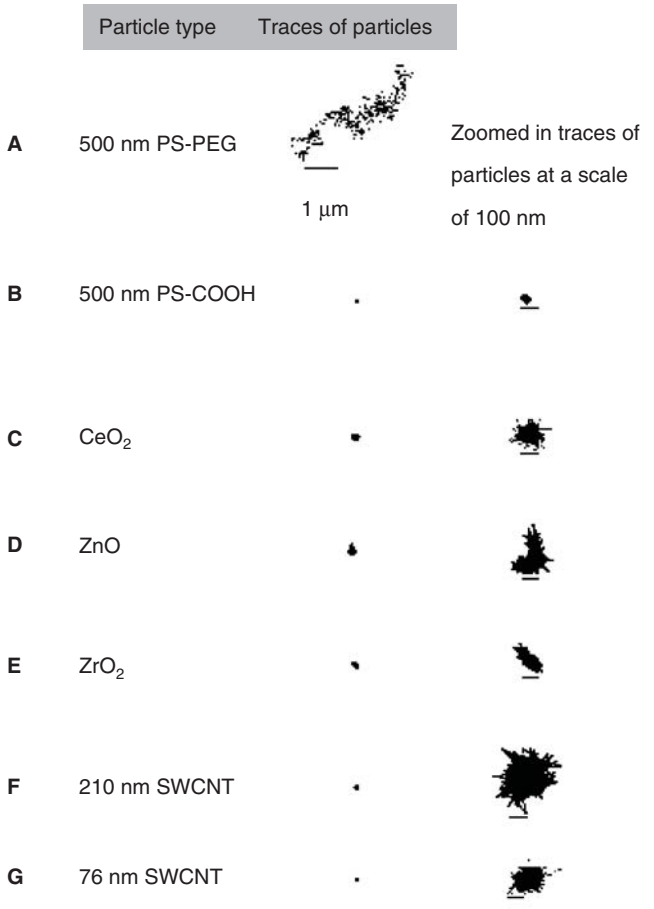

Figure 1. Representative 20 s time-lapse traces of fluorescent metal oxide nanoparticles and single-walled carbon nanotubes (SWCNTs) in human mucus: (A) 500 nm PS-PEG (positive control), (B) 500 nm PS-COOH (negative control), (C) cerium oxide, CeO_2, (D) zinc oxide, ZnO, (E) zirconium dioxide, ZrO_2, (F) 210 nm SWCNT and (G) 76 nm SWCNT in neutralized human cervicovaginal mucus.

limit over a typical 8 h workday. Assuming that this mass dose is uniformly distributed over the surface area of the tracheobronchial region (2471 cm^2; Mercer et al. 1994), the mass dose per epithelial surface area of ZnO is ~0.2 $\mu g/cm^2$ (380 $\mu g \div 2471\ cm^2$). Using the same approach, we estimated that ~175 μg (0.3% × 58 mg or mass per surface area dose of ~0.1 $\mu g/cm^2$) of CeO_2 may penetrate the mucus lining the tracheobronchial airways and interact with the underlying epithelial cells.

Cellular uptake of nMeOs and SWCNTs

We quantified the uptake of fluorescent nMeOs and SWCNTs by human bronchial epithelial cells after a 4 h exposure using FCM. CeO_2 and ZrO_2 particles were internalized more efficiently than smaller ZnO particles; the percentages of BEAS-2B cells with fluorescent nMeOs after 4 h were ~60% for CeO_2, ~30% for ZnO and ~75% for ZrO_2 (Figure 4). We found minimal differences in the uptake for both 210 and 76 nm SWCNTs at a mass dose of 1 μg (Figure 4); for both SWCNT lengths, ~98% cells internalized SWCNTs within 4 h.

Effects of nMeOs and SWCNTs on cell viability

ZnO markedly reduced cell viability at doses ~10 μg/ml and higher, with an LC_{50} of ~15 μg/ml (10 $\mu g/cm^2$) (approximated between concentrations of 10 and 20 μg/ml) (Figure 5A). Since ~2% of ZnO particles may penetrate a relevant distance in human mucus within 1 h, we estimated that the mass per area dose to the tracheobronchial epithelium for ZnO is ~0.2 $\mu g/cm^2$ (2% × 10 $\mu g/cm^2$). Human bronchial epithelial cells, upon treatment with ZnO, were affected at doses as low as 10 $\mu g/cm^2$, which is ~50-fold higher than the dose expected to be available to the tracheobronchial epithelium. CeO_2 did not affect cell viability at all concentrations tested. ZrO_2 affected human bronchial epithelial cell viability at concentrations ≥30 μg/ml (mass per area dose of ~20 $\mu g/cm^2$). However, our model of particle penetration suggests that only a negligible fraction of ZrO_2 particles may reach the mucosal epithelium.

We tested the effects of SWCNTs on cell viability at doses from 100 to 400 μg/ml (25, 50 and 100 $\mu g/cm^2$). Longer SWCNTs (210 nm) affected cell viability at 200 and 400 μg/ml doses while shorter SWCNTs (76 nm) only affected viability at 400 μg/ml dose. (Figure 5B). Table II lists the hydrodynamic diameters and ζ-potentials for CeO_2, ZnO and ZrO_2, measured in cell culture medium. The sizes of nMeOs in cell culture medium were 382 ± 48, 379 ± 13 and 470 ± 13 nm for CeO_2, ZnO and ZrO_2 respectively. The ζ-potentials for CeO_2, ZnO and ZrO_2 in cell culture medium were −11 ± 1, −10 ± 1 and −9.0 ± 0.5, respectively.

Discussion

A routine assumption in pulmonary toxicology is that inhaled nanoparticles will reach and directly interact with the airway epithelium. Nevertheless, we found that, with the exception of a small fraction of ZnO particles, nMeOs and SWCNTs tested were effectively immobilized by mucus, thereby greatly limiting the flux of particles that is expected to reach the tracheobronchial epithelium. Even for ZnO particles, of the 19 mg that are expected to deposit in the tracheobronchial region of the lung for individuals exposed at the daily OSHA limit, we estimate that only 0.4 mg (~0.2 $\mu g/cm^2$) may diffuse fast enough to reach the epithelium. While the small fraction of fast-moving outlier nanoparticles and substantial toxicity of ZnO suggests that their risk for pulmonary toxicity should be investigated further, these findings underscore the apparent effectiveness of the protective barrier function of mucus. Our findings suggest that prior studies of toxicity of nanomaterials to lung epithelium may overestimate the dose of nanomaterials that reach cells.

Foreign particles can become immobilized in mucus by steric hindrance from the dense mucin mesh, or by adhesive interactions with mucus constituents. We recently found that the average pore diameter of human CVM secretions is ~340 nm, with a substantial fraction of pores larger than 500 nm, which allows 500 nm 'muco-inert' PS-PEG particles to undergo rapid diffusion (Lai et al. 2007, 2010). Thus, it is unlikely that the nMeOs tested here are trapped by steric hindrance alone. Instead, the particles tested likely adhere to mucus constituents via electrostatic attractions, hydrogen bonding and/or hydrophobic interactions. Since most metal

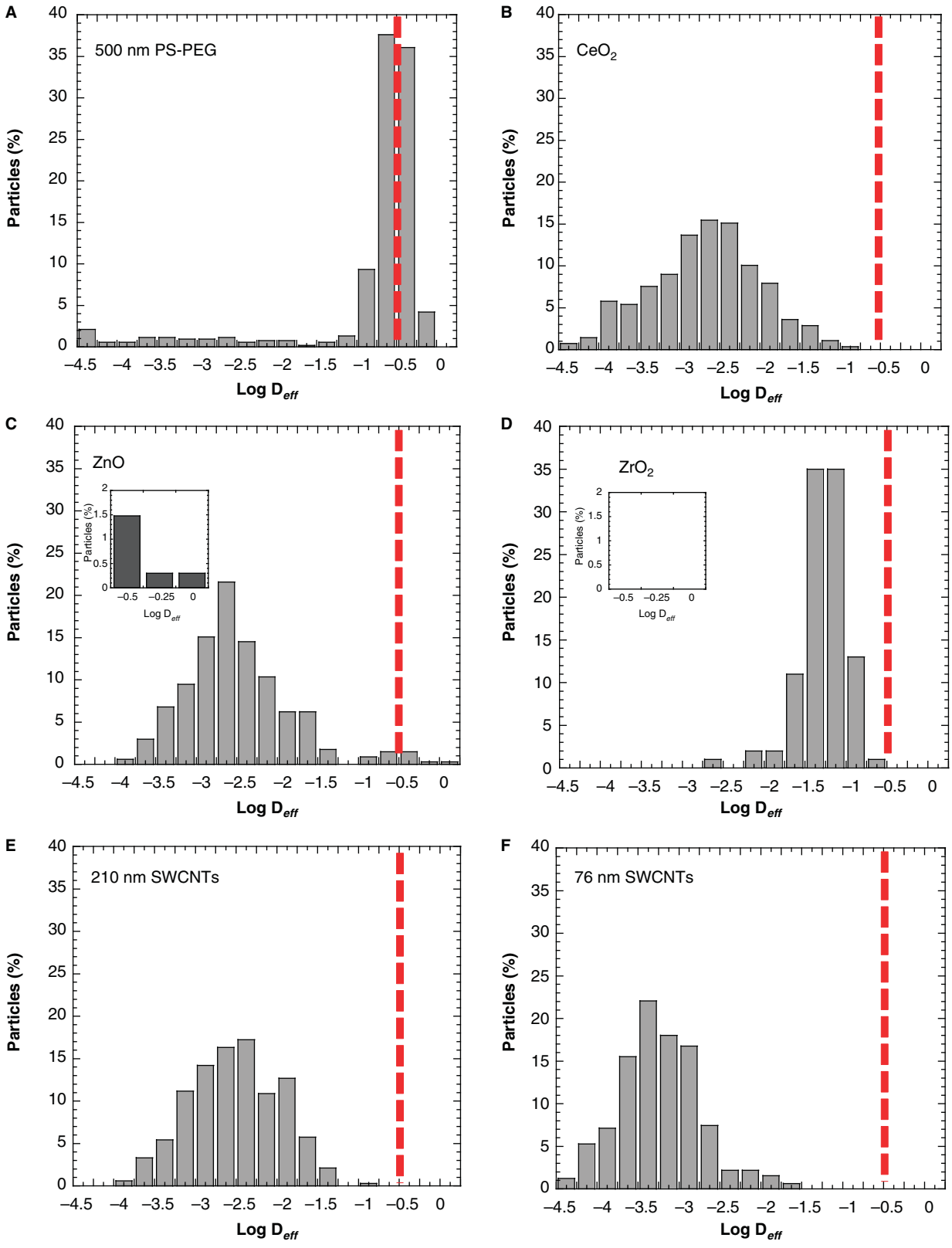

Figure 2. Diffusion of metal oxide nanoparticles (nMeOs) and single-walled carbon nanotubes (SWCNTs) in human mucus. Distributions of the logarithms of individual particle-effective diffusivities (D_{eff} at τ = 1 s) for (A) 500-nm PS-PEG, (B–D) nMeOs and (E–F) SWCNTs.

oxide surfaces are hydrophobic (Li & Logan 2004; Meng et al. 2006), nMeOs are likely immobilized in mucus by interactions with hydrophobic domains interspersed along mucin fibres, similar to hydrophobic polystyrene particles (Lai et al. 2007, 2010). The greater mobility of ZnO may be attributed to their smaller size, which reduces not only the surface area per particle available for mucoadhesive interactions, but also the probability of a ZnO particle encountering multiple mucin fibres simultaneously.

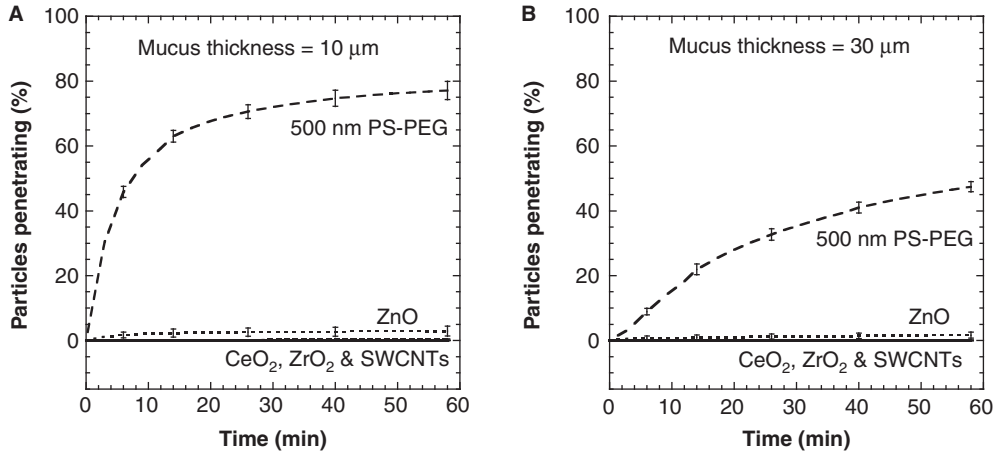

Figure 3. Penetration of metal oxide nanoparticles (nMeOs) and single-walled carbon nanotubes (SWCNTs) across human mucus over time. Particles are assumed to be uniformly deposited in airway lumen on top of the mucus layer and must penetrate the mucus layer to reach underlying epithelial cells. Speeds of individual particles were obtained from particle-tracking data by projecting the measured mean-squared displacement versus τ relationship to long times. Concentration profiles over time were obtained by numerically integrating Fick's second law: (A) particle penetration over time for nMeOs and SWCNTs across mucus layer thickness of 10 μm; (B) particle penetration over time for nMeOs and SWCNTs across mucus layer thickness of 30 μm.

Although conjugation of fluorophores to particles was necessary to visualize their mobility, we considered that covalent conjugation of fluorophores to the nanoparticle surface may cause artefactual trapping of nanoparticles in mucus via potential flurophore–mucin adhesive interactions. Thus, we utilized labelling methods that have been widely adapted for studying biological behaviour and response of engineered nanoparticles, including the study of nanoparticle penetration of human mucus. Specifically, FITC was used as the fluorophore, since conjugation of FITC to Norwalk virus and human papillomavirus did not reduce the mobility of these viruses in human cervical mucus, suggesting that FITC is essentially muco-inert (Olmsted et al. 2001). Since FITC did not cause viral particles to adhere to mucus, it is highly unlikely that FITC labelling could be responsible for the observed nanoparticle trapping in human mucus observed here. Instead, the forces that cause the nanoparticles to bind to mucus most likely arise from interactions between mucins and regions of particle surface not coated with FITC. Thus, it is expected that unlabeled nanoparticles will be immobilized in human mucus to the same extent as the labelled particles in our study. This is likely a unique property of the adhesive interactions that immobilize particles in mucus: it only takes a small number of weak bonds to immobilize particles in mucus with permanent avidity. Hence, partial coverage of the surface of particles that are mucoadhesive with a muco-inert molecule will not prevent particles from becoming immobilized in mucus.

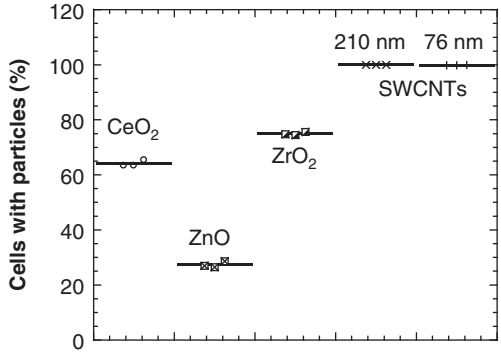

Figure 4. Uptake of fluorescent metal oxide nanoparticles (nMeOs) and single-walled carbon nanotubes (SWCNTs) by human bronchial epithelial (BEAS-2B) cells. BEAS-2B cells were treated with 1 μg of fluorescent nMeOs and SWCNTs for 4 h and particle uptake was determined using flow cytometry. Three independent experiments were performed.

Exposure calculations indicate that an individual inhaling SWCNTs may be exposed to a mass per area dose of ~0.1 μg/cm^2 in the tracheobronchial airways. This suggests that the doses at which we investigated human bronchial epithelial cell viability were at least 250 to 1000 fold higher ($25 \div 0.1$ μg/cm^2 or $100 \div 0.1$ μg/cm^2) than what the effective dose the airways of an individual exposed to SWCNTs would likely encounter, even if we do not account for the mucus barrier. Since our model of particle penetration suggests that few SWCNTs can penetrate physiologically thick mucus layers, the effective dose reaching the airway epithelium is likely even less. Although human bronchial epithelial cells readily internalize both lengths of SWCNTs, we found only a negligible fraction of SWCNTs penetrate human mucus. Since SWCNTs at doses of ~250 to 1000 fold greater than quantities that would likely deposit in the tracheobronchial airways only produced a modest decline in cell viability, their risks for causing toxicity in the mucus-covered regions of the lung airways is likely limited.

Since the length of SWCNTs studied here are smaller than the pore sizes in mucus, SWCNTs are also likely slowed by adhesive rather than steric interactions. Dawson et al. found that coating polymeric nanoparticles with DNA increased their mobility in reconstituted gastric mucus ~10-fold compared with similarly sized uncoated polymeric particles (Dawson et al. 2003), suggesting that a DNA coating may reduce the mucoadhesion of SWCNTs. It is possible that the surfaces of SWCNTs, although wrapped with hydrophilic ssDNA, may still have exposed hydrophobic regions (Chen et al. 2001; Arnold et al. 2006; Dong et al. 2008;

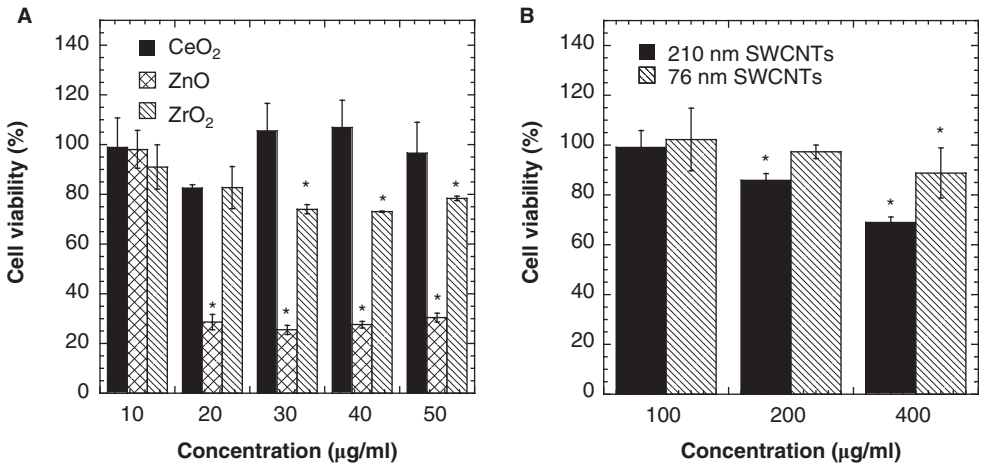

Figure 5. Effect of metal oxide nanoparticles (nMeOs) and single-walled carbon nanotubes (SWCNTs) on human bronchial epithelial cell viability after 24 h: (A) nMeOs and (B) SWCNTs. Data represents mean + SEM of three experiments, performed in triplicates. Statistical significance (*) comparing treatments with non-treated cells is determined using a one-tailed Student's *t*-test with $p < 0.05$.

Manivannan et al. 2009) that can associate with mucins via polyvalent-adhesive interactions. This explanation is supported by our earlier observation that as little as a 40% reduction in PEG-coating density caused particles to be slowed in mucus by 700-fold (Wang et al. 2008).

The cellular toxicity of ZnO particles may be attributed to increased production of ROS (Xia et al. 2008), where the generation of oxygen radicals have been implicated in a variety of respiratory tract disorders (Barnes 1990; Cross et al. 1994). It has been shown that ZnO increases the production of oxygen radicals from human neutrophils (Lindahl et al. 1998), which may contribute to the pathogenesis of zinc fume fever (Kaye et al. 2002). ZnO nanoparticles have also been shown to increase TNF-α, IL-6 and IL-8 production, which can lead to metal fume fever in welders (Xia et al. 2008). Recent work has shown that low doses of SWCNTs can perturb the transepithelial electrical resistance (TEER) in cocultures of primary human bronchial epithelial cells and fibroblasts (Stoker et al. 2008). In these experiments, the TEER value was dramatically decreased post-exposure to SWCNTs, implying that SWCNTs markedly reduced the barrier function of airway epithelial cell layers. Although we did not investigate the toxicity of nMeOs and SWCNTs to cell characteristics of the alveolar region in the human respiratory tract, it is possible that engineered nanoparticles may induce toxicological responses in the alveolar region as evident in rodent studies of ultrafine titanium dioxide (TiO_2) and CNTs (Lam et al. 2004; Warheit et al. 2004; Shvedova et al. 2005). The alveolar region may be particularly susceptible to damage induced by toxic nanomaterials since, unlike the airways, alveoli are not protected by a mucus blanket.

Table II. Physicochemical properties of metal oxide nanoparticles.

Particle	Dimension measured	Dimensions of nanoparticles (nm)	ζ-Potential of nanoparticles (mV)
CeO_2*	Diameter	382 ± 48	−11 ± 1
ZnO*	Diameter	379 ± 13	−10 ± 1
ZrO_2*	Diameter	470 ± 13	−9.0 ± 0.5

*Size and ζ-potentials of particles measured in cell culture media.

In conclusion, human mucus is a critical diffusional barrier that may offer significant protection of the airways against inhaled engineered nanoparticles. Our findings challenge the common assumption that inhaled particles will reach and directly interact with epithelial cells, since the mucus layer will greatly reduce the flux of most particles to underlying tissues. Our work underscores the importance and need to improve our understanding of particle–mucus interactions for a wide range of engineered and environmental nanoparticles.

Acknowledgements

This work was supported by the NIH/NIEHS (P50ES015903), NSF (CBET-0837946), NIEHS Center Grant 2 P30 ES003819 and NIEHS Training Grant T32 ES007141.

Declaration of interest

The authors report no conflicts of interest. The authors alone are responsible for the content and writing of the paper.

References

Arnold MS, Green AA, Hulvat JF, Stupp SI, Hersam MC. 2006. Sorting carbon nanotubes by electronic structure using density differentiation. Nat Nanotechnol 1:60–65.

Barnes PJ. 1990. Reactive oxygen species and airway inflammation. Free Radic Biol Med 9:235–243.

Becker ML, Fagan JA, Gallant ND, Bauer BJ, Bajpai V, Hobbie EK, et al. 2007. Length-dependent uptake of DNA-wrapped single-walled carbon nanotubes. Adv Mater 19:939–945.

Boskey ER, Moench TR, Hees PS, Cone RA. 2003. A self-sampling method to obtain large volumes of undiluted cervicovaginal secretions. Sex Transm Dis 30:107–109.

Bottini M, Balasubramanian C, Dawson MI, Bergamaschi A, Bellucci S, Mustelin T. 2006. Isolation and characterization of fluorescent nanoparticles from pristine and oxidized electric arc-produced single-walled carbon nanotubes. J Phys Chem B 110:831–836.

Chen RJ, Zhang Y, Wang D, Dai H. 2001. Noncovalent sidewall functionalization of single-walled carbon nanotubes for protein immobilization. J Am Chem Soc 123:3838–3839.

Cone RA. 2009. Barrier properties of mucus. Adv Drug Deliv Rev 61:75–85.

Cross CE, Van Der Vliet A, O'neill CA, Eiserich JP. 1994. Reactive oxygen species and the lung. Lancet 344:930–933.
Dawson M, Krauland E, Wirtz D, Hanes J. 2004. Transport of polymeric nanoparticle gene carriers in gastric mucus. Biotechnol Prog 20:851–857.
Dawson M, Wirtz D, Hanes J. 2003. Enhanced viscoelasticity of human cystic fibrotic sputum correlates with increasing microheterogeneity in particle transport. J Biol Chem 278:50393–50401.
Deshpande S, Patil S, Kuchibhatla SVNT, Seal S. 2005. Size dependency variation in lattice parameter and valency states in nanocrystalline cerium oxide. Appl Phys Lett 87:133113.
Dong L, Joseph KL, Witkowski CM, Craig MM. 2008. Cytotoxicity of single-walled carbon nanotubes suspended in various surfactants. Nanotechnology 19:1–5.
EPA. 1985. Development of statistical distributions or ranges of standard factors used in exposure assessments. In: NTIS, S,VA, editors. Washington, DC: Office of Health and Environmental Assessment.
Fernandez-Garcia M, Martinez-Arias A, Hanson JC, Rodriguez JA. 2004. Nanostructured oxides in chemistry: characterization and properties. Chem Rev 104:4063–4104.
Hirano S. 2009. A current overview of health effect research on nanoparticles. Environ Health Prev Med 14:223–225.
Hoet PH, Bruske-Hohlfeld I, Salata OV. 2004. Nanoparticles - known and unknown health risks. J Nanobiotechnol 2:12.
Kaye P, Young H, O'sullivan I. 2002. Metal fume fever: a case report and review of the literature. Emerg Med J 19:268–269.
Kisin ER, Murray AR, Keane MJ, Shi XC, Schwegler-Berry D, Gorelik O, et al. 2007. Single-walled carbon nanotubes: geno- and cytotoxic effects in lung fibroblast V79 cells. J Toxicol Environ Health A 70:2071–2079.
Kleinstreuer C, Zhang Z. 2010. Airflow and particle transport in the human respiratory system. Annu Rev Fluid Mech 42:301–334.
Lai SK, O'hanlon DE, Harrold S, Man ST, Wang YY, Cone R, Hanes J. 2007. Rapid transport of large polymeric nanoparticles in fresh undiluted human mucus. Proc Natl Acad Sci USA 104:1482–1487.
Lai SK, Wang YY, Hida K, Cone R, Hanes J. 2010. Nanoparticles reveal that human cervicovaginal mucus is riddled with pores larger than viruses. Proc Natl Acad Sci USA 107:598–603.
Lam CW, James JT, Mccluskey R, Hunter RL. 2004. Pulmonary toxicity of single-wall carbon nanotubes in mice 7 and 90 days after intratracheal instillation. Toxicol Sci 77:126–134.
Li B, Logan BE. 2004. Bacterial adhesion to glass and metal-oxide surfaces. Colloids Surf B Biointerfaces 36:81–90.
Li Q, Chen SL, Jiang WC. 2007. Durability of nano ZnO antibacterial cotton fabric to sweat. J Appl Polym Sci 103:412–416.
Lindahl M, Leanderson P, Tagesson C. 1998. Novel aspect on metal fume fever: zinc stimulates oxygen radical formation in human neutrophils. Hum Exp Toxicol 17:105–110.
Liu B, Ren W, Liu C, Sun CH, Gao L, Li S, et al. 2009. Growth velocity and direct length-sorted growth of short single-walled carbon nanotubes by a metal-catalyst-free chemical vapor deposition process. ACS Nano 3:3421–3430.
Lucente-Schultz RM, Moore VC, Leonard AD, Price BK, Kosynkin DV, Lu M, et al. 2009. Antioxidant single-walled carbon nanotubes. J Am Chem Soc 131:3934–3941.
Manivannan S, Jeong IO, Ryu JH, Lee CS, Kim KS, Jang J, Park KC. 2009. Dispersion of single-walled carbon nanotubes in aqueous and organic solvents through a polymer wrapping functionalization. J Mater Sci Mater Electronics 20:223–229.
Markovic B, Rerek ME. 2002. Properties of nanosized particles in sunscreen formulations. Abstr Pap Am Chem Soc 223:U439-U439.
Maynard AD, Baron PA, Foley M, Shvedova AA, Kisin ER, Castranova V. 2004. Exposure to carbon nanotube material: aerosol release during the handling of unrefined single-walled carbon nanotube material. J Toxicol Environ Health A 67:87–107.
Meng S, Zhang Z, Kaxiras E. 2006. Tuning solid surfaces from hydrophobic to superhydrophilic by submonolayer surface modification. Phys Rev Lett 97:036107.
Mercer RR, Russell ML, Roggli VL, Crapo JD. 1994. Cell number and distribution in human and rat airways. Am J Respir Cell Mol Biol 10:613–624.
Nel A, Xia T, Madler L, Li N. 2006. Toxic potential of materials at the nanolevel. Science 311:622–627.
Niyogi S, Hu H, Hamon MA, Bhowmik P, Zhao B, Rozenzhak SM, et al. 2001. Chromatographic purification of soluble single-walled carbon nanotubes (s-SWNTS). J Am Chem Soc 123:733–734.
Olmsted SS, Padgett JL, Yudin AI, Whaley KJ, Moench TR, Cone RA. 2001. Diffusion of macromolecules and virus-like particles in human cervical mucus. Biophys J 81:1930–1937.
Pacurari M, Yin XJ, Zhao J, Ding M, Leonard SS, Schwegler-Berry D, et al. 2008. Raw single-wall carbon nanotubes induce oxidative stress and activate MAPKs, AP-1, NF-kappaB, and Akt in normal and malignant human mesothelial cells. Environ Health Perspect 116:1211-1217.
Padmavathy N, Vijayaraghavan R. 2008. Enhanced bioactivity of ZnO nanoparticles-an antimicrobial study. Sci Technol Adv Mater 9:1–7.
Papaspyridakos P, Lal K. 2008. Complete arch implant rehabilitation using subtractive rapid prototyping and porcelain fused to zirconia prosthesis: a clinical report. J Prosthet Dent 100:165–172.
Risom L, Moller P, Loft S. 2005. Oxidative stress-induced DNA damage by particulate air pollution. Mutat Res 592:119–137.
Shi X, Hudson JL, Spicer PP, Tour JM, Krishnamoorti R, Mikos AG. 2006. Injectable nanocomposites of single-walled carbon nanotubes and biodegradable polymers for bone tissue engineering. Biomacromolecules 7:2237–2242.
Shi X, Sitharaman B, Pham QP, Liang F, Wu K, Edward Billups W, et al. 2007. Fabrication of porous ultra-short single-walled carbon nanotube nanocomposite scaffolds for bone tissue engineering. Biomaterials 28:4078–4090.
Shvedova AA, Fabisiak JP, Kisin ER, Murray AR, Roberts JR, Tyurina YY, et al. 2008a. Sequential exposure to carbon nanotubes and bacteria enhances pulmonary inflammation and infectivity. Am J Respir Cell Mol Biol 38:579–590.
Shvedova AA, Kisin E, Murray AR, Johnson VJ, Gorelik O, Arepalli S, et al. 2008b. Inhalation vs. aspiration of single-walled carbon nanotubes in C57BL/6 mice: inflammation, fibrosis, oxidative stress, and mutagenesis. Am J Physiol Lung Cell Mol Physiol 295:L552–L565.
Shvedova AA, Kisin ER, Mercer R, Murray AR, Johnson VJ, Potapovich AI, et al. 2005. Unusual inflammatory and fibrogenic pulmonary responses to single-walled carbon nanotubes in mice. Am J Physiol Lung Cell Mol Physiol 289:L698–L708.
Sinnott SB, Andrews R. 2001. Carbon nanotubes: synthesis, properties, and applications. Crit Rev Solid State Mater Sci 26:145–249.
Sitharaman B, Shi X, Tran LA, Spicer PP, Rusakova I, Wilson LJ, Mikos AG. 2007. Injectable in situ cross-linkable nanocomposites of biodegradable polymers and carbon nanostructures for bone tissue engineering. J Biomater Sci Polym Ed 18:655–671.
Stoker E, Purser F, Kwon S, Park YB, Lee JS. 2008. Alternative estimation of human exposure of single-walled carbon nanotubes using three-dimensional tissue-engineered human lung. Int J Toxicol 27:441–448.
Subramoney S. 1998. Novel nanocarbons - Structure, properties, and potential applications. Adv Mater 10:1157–1171.
Suh J, Dawson M, Hanes J. 2005. Real-time multiple-particle tracking: applications to drug and gene delivery. Adv Drug Deliv Rev 57:63–78.
Suh J, Wirtz D, Hanes J. 2003. Efficient active transport of gene nanocarriers to the cell nucleus. Proc Natl Acad Sci USA 100:3878–3882.
Tang BC, Dawson M, Lai SK, Wang YY, Suk JS, Yang M, et al. 2009. Biodegradable polymer nanoparticles that rapidly penetrate the human mucus barrier. Proc Natl Acad Sci USA 106:19268–19273.
Verkman AS, Song Y, Thiagarajah JR. 2003. Role of airway surface liquid and submucosal glands in cystic fibrosis lung disease. Am J Physiol Cell Physiol 284:C2–C15.
Wang YY, Lai SK, Suk JS, Pace A, Cone R, Hanes J. 2008. Addressing the PEG mucoadhesivity paradox to engineer nanoparticles that "Slip" through the human mucus barrier. Angew Chem Int Ed 47:9726–9729.
Warheit DB, Laurence BR, Reed KL, Roach DH, Reynolds GA, Webb TR. 2004. Comparative pulmonary toxicity assessment of single-wall carbon nanotubes in rats. Toxicol Sci 77:117–125.
Xia T, Kovochich M, Liong M, Madler L, Gilbert B, Shi H, et al. 2008. Comparison of the mechanism of toxicity of zinc oxide and cerium oxide nanoparticles based on dissolution and oxidative stress properties. ACS Nano 2:2121–2134.
Zheng M, Jagota A, Semke ED, Diner BA, Mclean RS, Lustig SR, et al. 2003a. DNA-assisted dispersion and separation of carbon nanotubes. Nat Mater 2:338–342.
Zheng M, Jagota A, Strano MS, Santos AP, Barone P, Chou SG, et al. 2003b. Structure-based carbon nanotube sorting by sequence-dependent DNA assembly. Science 302:1545–1548.